Cell-attached patch clamp study of the electropermeabilization of amphibian cardiac cells

Rory J. O'Neill and Leslie Tung
Department of Biomedical Engineering, The Johns Hopkins University School of Medicine, Baltimore, Maryland 21205 USA

ABSTRACT Potential gradients imposed across cell or lipid membranes break down the insulating properties of these barriers if an intensity and time-dependent threshold is exceeded. Potential gradients of this magnitude may occur throughout the body, and in particular in cardiac tissue, during clinical defibrillation, ablation, and electrocution trauma. To study the dynamics of membrane electropermeabilization a cell-attached patch clamp technique was used to directly control the potential across membrane patches of single ventricular cells enzymatically isolated from frog (*Rana pipiens*) hearts. Ramp waveshapes were used to reveal rapid membrane conductance changes that may have otherwise been obscured using rectangular waveshapes. We observed a step increase ($\Delta t < 30$ μs) or *breakdown* in membrane conductance at transmembrane potential thresholds of 0.6–1.1 V in response to 0.1–1.0 kV/s voltage ramps. Conductance kinetics on a sub-millisecond time scale indicate that breakdown is preceded by a period of instability during which the noise and amplitude of the membrane conductance begin to increase. In some cells membrane breakdown was observed to be fully reversible when using an intershock interval of 1 min (20–23°C). These findings support energetic models of membrane electropermeabilization which describe the formation of membrane pores (or growth of existing pores) to a conducting state (*instability*), followed by a rapid expansion of these pores when the energy barrier for the formation of hydrophilic pores is overcome (*breakdown*).

INTRODUCTION

Electrically related mechanisms are responsible for the pathological consequences of high intensity electrical shock received by the body during clinical defibrillation (Tacker and Geddes, 1980; Jones et al., 1987; Tung, 1990), clinical ablation (Bardy and Sawyer, 1990), and in electrocution accidents (Bhatt et al., 1990). An extracellular electric field of ~1.3 V/cm is sufficient for stimulation of the heart (Frazier et al., 1988) and in terms of (induced) transmembrane potential, a 25 mV depolarization is the accepted value for cardiac tissue excitation (Krassowska et al., 1990). Since the electric field in the heart during defibrillation can exceed 60 V/cm (transthoracic defibrillation estimations, Lepeschkin et al., 1980; internal defibrillation measurements, Yabe et al., 1990), by simple extension volt-level transmembrane potentials could be induced in individual cardiac cells. It has been shown in cell and lipid bilayer membranes that transmembrane potentials of this magnitude cause the formation of reversible, nonspecific pathways for ions and molecules (i.e., pores), which dramatically increase the membrane conductance and permeability (Zimmermann, 1986; Neumann, 1989). Electroporation and electropermeabilization are two terms used to describe the transient enhanced permeability state of cell and liquid bilayer membranes in response to the application of electric fields. Electroporation has been applied as a technique in place of microinjection and chemical transport to introduce molecules and compounds into cells for biochemical and genetic expression studies (Chassy and Flickinger, 1987; Dower et al., 1988), and for drug delivery (Kinosita and Tsong, 1977; Zimmermann et al., 1980*a*).

Electropermeabilization is studied in membrane systems using two parameters: transmembrane potential and membrane permeability (or conductance). Transmembrane potential has been estimated from the applied extracellular electric field using electrostatic models (Kinosita and Tsong, 1979), and monitored directly using electrometer amplifiers (Benz and Zimmerman, 1980), potentiometric dye video microscopy (Gross et al., 1986; Kinosita et al., 1988), and the voltage clamp technique (Abidor et al., 1979; Chernomordik et al., 1987). Membrane permeability has been monitored via the flux of molecular probes, dyes, and radioactively labeled molecules (Serpersu et al., 1985; Sowers and Lieber, 1986; Mir et al., 1988; Mehrle et al., 1989), by colloid-osmotic lysis and release of intracellular constituents (Riemann et al., 1975; Kinosita and Tsong, 1979; Mir et al., 1988; Deuticke and Schwister, 1989), release of fluorescent labeled molecules (Jones et al., 1987; Bliss

Address correspondence to Leslie Tung, Department of Biomedical Engineering, The Johns Hopkins University School of Medicine, 720 Rutland Ave., Baltimore, MD 21205.

0006-3495/91/05/1028/12 $2.00

et al., 1988), and cell contracture (Lee et al., 1988; Mulligan et al., 1988). Ultrastructural changes have been documented using electron microscopy in cultured heart cells (Jones et al., 1980), ovary cells (Escande-Géraud et al., 1988), human erythrocytes (Chang and Reese, 1990), and other cultured cells (Gass and Chernomordik, 1990). Membrane conductance has been monitored using the charge-pulse relaxation technique (Benz and Zimmermann, 1980; see Benz and Conti, 1981*b* for description), the modified Coulter cell counter technique (Zimmermann et al., 1981), cell suspension conductivity (Kinosita and Tsong, 1979), lipid bilayer conductivity (Glaser et al., 1988), and single-cell membrane conductivity using the patch clamp method (Chernomordik et al., 1987).

The study of electrically induced cell membrane permeabilization in various tissue types is important because of the frequent occurrence of the application of electrical shock to body tissues either clinically or during electrical trauma. The importance of the characterization of electropermeabilization in cardiac cell membranes is underscored by the likelihood that high energy shock received by the myocardium clinically or during electrocution could induce life threatening dysfunction. The electrophysiological consequences of the loss of the barrier functions of the cardiac cell membrane as a result of membrane breakdown or rupture include decreased resting potential, decreased conduction velocity, elevated excitation threshold, and arrhythmias (Jones et al., 1978; Tung, 1990). In heart tissue there are two additional considerations: (*a*) any positive mechanical tension imposed on the cell membrane, such as occurs in situ to heart cells during the cardiac cycle, may lower the threshold potential required for membrane breakdown (Zimmermann et al., 1977; Needham and Hochmuth, 1989) and (*b*) heart cells are electrically coupled which increases the effective cell length; because the induced transmembrane potential due to an external electric field increases as a function of cell length parallel to the electric field axis (Klee and Plonsey, 1976; Jeltsch and Zimmerman, 1979), field-induced transmembrane potentials may be greater in cardiac tissue than in other (electrically uncoupled) tissue types (Tung, 1990).

The goals of this study were to demonstrate that electrically induced membrane breakdown occurs in isolated cardiac cells and to identify the predominant characteristics of this phenomenon. A cell-attached patch clamp technique was used to directly control the potential of membrane patches in single ventricular cells that were enzymatically isolated from frog (*Rana pipiens*) hearts. These results have been presented in part in abstract form (O'Neill and Tung, 1989; Tung and O'Neill, 1990).

MATERIALS AND METHODS

I. Single cell preparation

Single viable ventricular cells were obtained from whole frog hearts via enzymatic dissociation. Amphibian ventricular cells are spindle-like in structure having tapered ends with overall dimensions of 200–400 μm long, 10–20 μm wide, and 2–5 μm thick. Viable hearts were excised from adult *Rana pipiens* frogs (Carolina Biological Supply, Burlington, NC or West Jersey Biological, Wenonah, NJ) and retrograde prefused through the aorta with three solutions: (*a*) 1.0 mM Ca^{2+} Ringer's (110 mM NaCl, 3 mM KCl, 10 mM Hepes) (23°C) for 15 min; (*b*) nominally zero Ca^{2+} Ringer's (23°C) for 45 min; and (*c*) enzyme solution (11 mg albumin [Fraction I; Sigma Chemical Co., St. Louis, MO], 13 mg collagenase [Type IA; Sigma Chemical Co.], 2 mg protease [Type XIV; Sigma Chemical Co.] in 25 ml nominally zero Ca^{2+} Ringer's) (30°C) for 10–25 min depending on the size of the heart (Mitra and Morad, 1985). Cells were stored refrigerated in 0.2 mM Ca^{2+} Ringer's solution and remained viable for over 10 h.

II. Voltage clamp amplifier and instrumentation

The cell-attached patch clamp method was used to measure the change in membrane patch conductance in response to DC voltage pulses. The lid of a 35-mm diam plastic tissue culture dish served as the experimental chamber which contained the bath solution and the Ag-AgCl driven-bath electrode for the patch clamp amplifier. Glass pipette microelectrodes were prepared using capillary tubes (Kimax-51; Kimble Products, Toledo, OH) on a vertical pipette puller (#720; David Kopf Instruments, Tujunga, CA). Resistances of the pipettes filled with 100 Ω-cm electrolyte ranged from 2 to 20 MΩ. The glass microelectrodes were attached to the amplifier headstage using a suction pipette holder (#PC-S3; E. W. Wright, Guilford, CT) with suction being applied by mouth. The headstage transresistance amplifier performed current to voltage conversion across a 10 MΩ resistor using an electrometer op-amp (#AD546J; Analog Devices, Norwood, MA). The headstage was positioned in place using an XYZ motorized manipulator (Märzhäuser DC-3K micromanipulator, joystick control unit STM-3; Fine Science Tools, Belmont, CA).

A custom-built voltage clamp amplifier was driven by an auxiliary gating pulse and an auxiliary command potential. The auxiliary command signal was supplied by an analogue ramp generator circuit, which was later replaced by a microcomputer controlled 5 MHz 12-bit D/A waveform synthesizer (#INST-290; Cyber Research, New Haven, CT). Data was acquired and stored on 3.5'' floppy disks using a digital oscilloscope (#NIC 310; Nicolet Instrument, Madison, WI). Without frequency compensation the -3 dB bandwidth of the modified voltage clamp amplifier was 31 KHz, and the time resolution was 1–5 μs depending on the oscilloscope sampling rate. All patch clamp voltages reported in this paper were a measure of the potential of the pipette electrode relative to the driven bath electrode; the sense of electrical current traveling from the pipette to the bath was positive.

III. Experimental methods

All experiments were performed at standard atmospheric pressure and room temperature (20–23°C) on an inverted microscope (#TMS; Nikon, Garden City, NY) at 400–600X total magnification using Hoffman modulation contrast optics (Modulation Optics, Greenvale, NY). Freshly isolated cells or refrigerated cells that were allowed to reach room temperature were added to the experimental chamber. The investigation of the electropermeabilization of heart cell mem-

branes was conducted using two different cell-attached methods: macro-patch and micro-patch. The study was launched using the macro-patch method which was modeled after the experiments performed by Zimmerman et al. (1980*b*) in which cells were electropermeabilized as they passed through a modified Coulter cell counter device. The cells traveled one at a time through a small orifice which separated two electrolyte chambers, each containing a shock electrode. In our approach, ~5–15 μm of the tapered end of a cardiac cell was drawn into the mouth of the pipette electrode (Fig. 1, *upper right*). In this way the cell was obstructing the orifice which separated the pipette and bath electrolytes, each of which contained an Ag-AgCl shock electrode. The macro-patch voltage clamp technique offered high resolution, on-line tracking of the membrane conductivity as it changed in response to large electric fields (i.e., conductance kinetics). Also, the investigation of the effects of longer duration shocks was possible, whereas with the Coulter counter system the electrical insult had to be accomplished during the ~100 μs transit time of the cell. The macro-patch technique called for the use of pipette electrodes having aperture diameters of 2–3 μm at the tip ($R_{pipette}$ = 2–4 MΩ). Formation of the electrical membrane-pipette seal was monitored by sensing the current response to a 100 Hz train of 10 mV rectangular voltage pulses. We were only able to obtain seal resistances of 10–100 MΩ when using these relatively large diameter pipette tips. The transmembrane potential thresholds for changes in membrane conductance resulting from a variety of shock protocols were recorded.

The micro-patch method is the conventional patch clamp approach (Hamill et al., 1981) in which very small areas of membrane are studied and gigaohm level seal resistances are obtained (Fig. 1, *lower right*). With this method the leakage current through the membrane-electrode seal and its possible effect on the threshold potential for electropermeabilization could be eliminated. To prepare the electrodes, pipettes having aperture diameters of 3–6 μm at the tip were heat polished until the aperture diameter decreased to 0.2–1.0 μm ($R_{pipette}$ = 5–20 MΩ). Seal resistances of 100 to >1,000 MΩ were obtained, and potential thresholds for membrane conductance changes resulting from a variety of shock protocols were recorded. Referring to Fig. 1 we found that the purely capacitive pathway across the glass pipette wall contributed only a minor, constant offset in current as a result of the constant slope of the ramp pulse (see Fig. 5 legend). In both the macro-patch and micro-patch experiments the slight negative pressure applied to the pipette to establish a seal with the cell membrane was maintained during the conductance measurement.

Electrolyte compositions are identified in each figure with the following convention: concentration of the primary ions (millimolar) in the bath electrolyte//concentration of the primary ions (millimolar) in the pipette electrolyte. To suppress the effects of excitation and contraction of ventricular cells during our recordings, we employed two techniques: (*a*) in most of the experiments the cell membranes were depolarized to inactivate ion channels. Membrane depolarization was accomplished either electrically by applying a holding potential to match the cell's intrinsic resting potential, or chemically by immersing the cell in an intracellular-like electrolyte to balance the ion concentrations across the surface membrane, and (*b*) we employed shock durations of <20 ms to avoid the development of force (the mechanical latency for force development in amphibian cardiac cells is 20–80 ms [Winegrad, 1979]).

IV. Shock protocols

Following seal formation, positive and negative low amplitude (100 mV) voltage ramps were applied to assess the resistance and linearity of the seal. Then a standard 2 V ramp (either polarity) was applied to induce breakdown while the membrane conductance was recorded. The slopes of the DC ramps also were varied (0.1–1.0 kV/s) to investigate whether breakdown was strictly a *threshold* phenomenon or if the *rate of change* of the transmembrane potential played a role. In a few experiments we employed a ramp and hold waveform to elucidate further the time and voltage dependence of membrane breakdown.

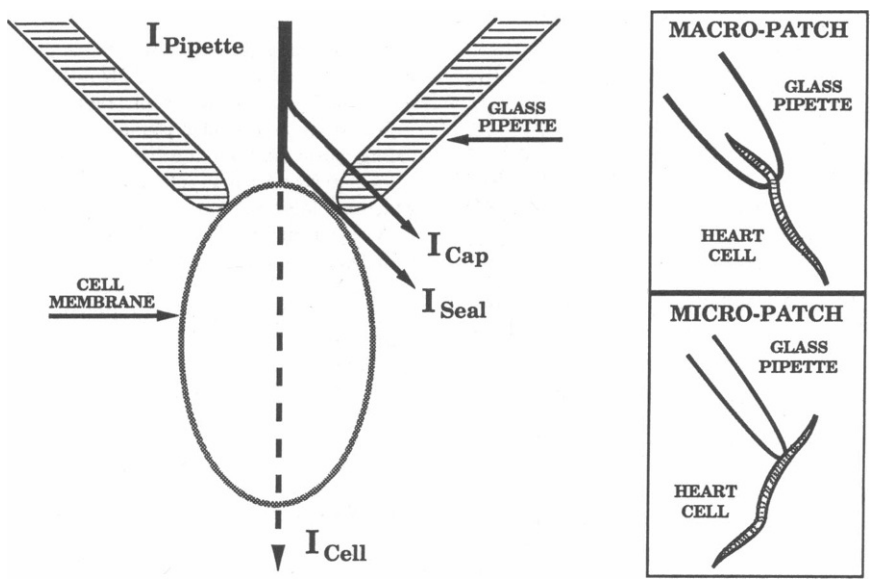

FIGURE 1 Electrical current pathways and patch types. There are three pathways for electrical current flow: (*a*) I_{Cap}, the purely capacitive pathway across the wall of the glass pipette, (*b*) I_{Seal}, the resistive leakage pathway formed between the cell membrane and the pipette tip, and (*c*) I_{Cell}, the electropermeabilization pathway through the cell. The two types of cell-attached patches used in this study were the *macro*-patch (*top right*) in which 10–15 μm of the cell end was drawn into the pipette, and the *micro*-patch (*bottom right*) or conventional patch clamp method.

RESULTS

The voltage clamp records of Fig. 2 depict the response of a cardiac cell membrane *macro*-patch to opposite polarity low amplitude voltage ramps (*upper traces*). The clamp currents (*lower traces*) are a direct measure of the membrane-pipette conductance. The behavior of the membrane patch was ohmic in response to these physiologic level (±100 mV) shocks. When the potential applied across the membrane macro-patch was increased 20-fold to 2 V we observed a much different response as shown for the two cells in Fig. 3. The predominant observation was the nonlinearity of the current in response to the large voltage ramps. The increased slope in each of the current traces corresponds to an increase in the membrane patch conductance. The general pattern of the response was similar for both polarities. Parameters of interest included the transmembrane potentials corresponding to the nonlinear changes in membrane conductance, the period of membrane instability preceding the step increase in conductances, and the transition time for the step increase.

The *micro*-patch protocol highlights the electrically induced changes in membrane conductance because the gigaohm level seals reduce the leakage currents to a negligible level. The conductance records of Fig. 4 were recorded from micro-patches in two different cells and demonstrate the sudden voltage-dependent increase in membrane conductance. We observed similar responses for both polarity shocks and the same types of response as for the macro-patch experiments.

The details of membrane conductance change during electropermeabilization are shown in Fig. 5 which is an enlargement from Fig. 4. The noisy, fluctuating increase in membrane conductance before the rapid step increase in conductance was observed in over 90% of the cells studied. The step increase in conductance consistently occurred over a 30 μs duration which corresponded to the bandwidth limitation of our system (~30 KHz). An overshoot of the conductance immediately following the jump increase was observed in ~80% of the cells exhibiting breakdown.

Since we did not know the conductance of the membrane proper (i.e., the nonpatch portion of the cell membrane) nor did we consistently measure the pipette tip resistance before mounting each cell, we could not determine the conductance of the membrane patch. However, a quantitative index of the conductance change of the membrane patch was defined by simply subtracting the initial system conductance (primarily a seal conductance) from the system conductance after electropermeabilization (measured during the ramp). This index was highly variable and ranged from 49.6 to 389 nS with a mean ± standard deviation of 230 ± 110 nS (n = 11) for the macro-patch experiments, and ranged from 11.5 to 373 nS with a mean ± standard deviation of 110 ± 79 nS (n = 32) for the micro-patch experiments. We could not quantitate further the change in patch conductance due to electropermeabilization or infer the number or sizes of pores in the patch from the total system conductance measurements because of the unknown conductance quantities mentioned above.

To determine whether the increase in membrane conductance resulting from electropermeabilization depended on fast ionic channels, Na^+ and Ca^{2+} channel blockers were employed. The conductance records of Fig. 6 are from two different cells, one bathed in an extracellular-like electrolyte (control), and the other in an extracellular-like electrolyte containing 10 μM TTX (a Na^+ channel blocker) and 1 mM $CdCl_2$ (a Ca^{2+} channel blocker). The membrane conductance responses for these two cells were similar, suggesting that membrane breakdown in amphibian cardiac cells does *not* involve the modulation of Na^+ and Ca^{2+} ionic channels.

To investigate the *reversibility* of electrically induced membrane breakdown, experiments were performed by applying suprathreshold 2 V ramps to the same mem-

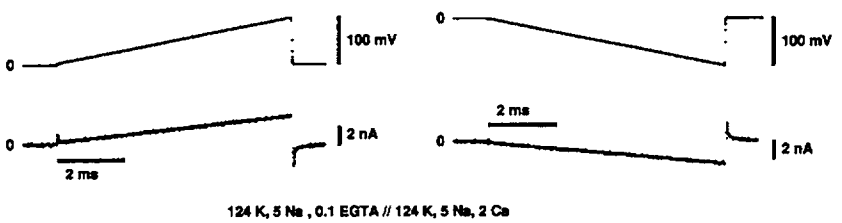

FIGURE 2 Low voltage ramps applied to a single membrane macro-patch. Opposite polarity 100 mV/7.0 ms voltage ramps (*upper traces*) were applied to the same *macro*-patch. The linearity and magnitude of the observed pipette current (*lower traces*) indicated that this was entirely a seal leakage current. Electrolyte compositions are identified as follows: *Primary ions in the* bath *electrolyte (millimolar)* // *Primary ions in the* pipette *electrolyte (millimolar)*. The measured seal conductance was 26.8 nS.

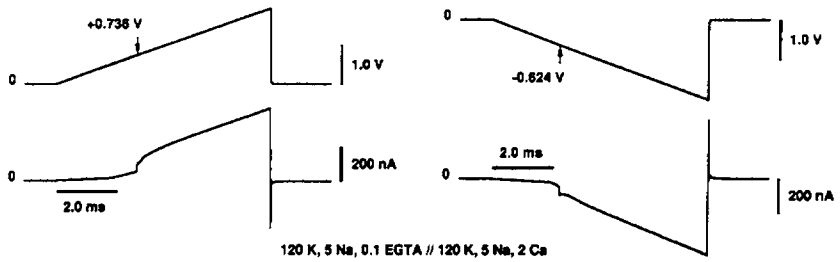

FIGURE 3 Volt-level ramps applied to membrane macro-patches. Two different cells were exposed to opposite polarity 2.0 V/7.0 ms ramps using the *macro*-patch protocol. The current traces (*lower waveforms*) show the sudden increase in membrane conductance which occurred at the threshold potentials noted on the voltage traces above. The structure of the positive and negative responses was observed to be both qualitatively and quantitatively similar. The conductance increased from 26.8 → 228 nS and 32.1 → 243 nS for the positive and negative polarity shocks, respectively.

brane patch with a 1 min intershock delay. In earlier multiple shock experiments a post-shock delay of 1 min almost always permitted the permeabilized patch conductance to decay to a steady-state value. The results are shown in Fig. 7 and in this case demonstrate the full recovery of the membrane patch between shocks. First the micro-patch was subjected to six consecutive −2 V/7 ms ramp shocks at the rate of 1 per min. The clamp currents preceding breakdown for all six shocks have similar slopes (i.e., conductance) indicating a restoration of the patch to its pre-shock condition. The seventh shock was applied within 15 s of the sixth shock; but in this case the membrane had *not* recovered based on the following observations: (*a*) the clamp current had a slope similar to those of the first six responses *after* breakdown, and (*b*) no abrupt increase in patch current occurred. Further investigation into the details of the time course of resealing at these temperatures (20–23°C) is being conducted in our lab (Tovar et al., 1990).

The ramp and hold command pulse of Fig. 8 was employed as a means of investigating whether electropermeabilization occurs strictly as a function of the *instantaneous* value of the transmembrane potential, or whether it is history dependent. In these experiments the membrane patch was subjected to a subthreshold ramp followed immediately by a DC holding potential corresponding to the maximum ramp potential. Indeed, abrupt changes in membrane conductance of the type observed previously in response to volt-level ramp pulses (Figs. 3–7) were observed to occur during the DC holding potential. Membrane electropermeabilization occurred at holding potentials in the range of 0.40–1.01 V, for four cells bathed in an intracellular-like electrolyte.

Table 1 summarizes the mean breakdown thresholds for the macro- and micro-patch protocols for a variety of electrolyte combinations. The data in this table were restricted to the *first* suprathreshold shock applied to the membrane patch; subsequent shocks applied to the patch were not always regulated in interval of occur-

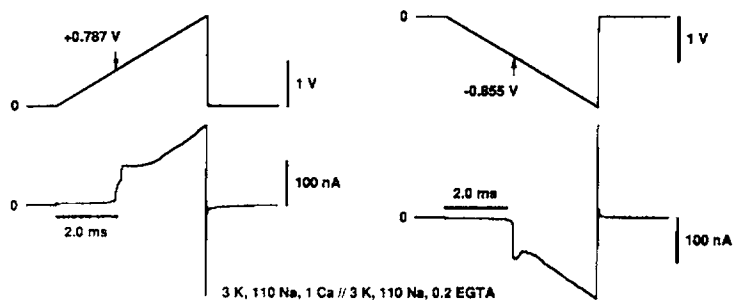

FIGURE 4 Volt-level ramps applied to membrane micro-patches. Two different cells were exposed to opposite polarity 2.0 V/7.0 ms ramps using the *micro*-patch protocol. The current traces (*lower waveforms*) show a minimal leakage current as a result of attaining gigaohm level seals. Here again we observed the positive and negative current responses to be qualitatively and quantitatively similar, and note that the qualitative structure was the same as that for the *macro*-patch results. The threshold breakdown potentials are noted on the voltage traces (*upper waveforms*); the conductance increases were 0.97 → 121 nS and 2.2 → 143 nS for the positive and negative shocks, respectively.

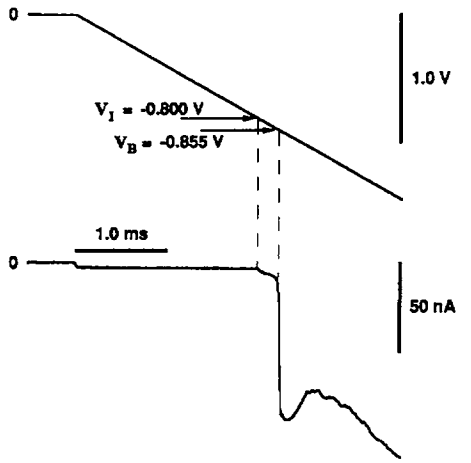

FIGURE 5 Details of frog cardiac membrane electropermeabilization. An examination of the dynamics of changes in patch conductance, taken from Fig. 4. The first threshold encountered in response to the −2.0 V/7.0 ms ramp was that of *membrane instability* occurring at voltage V_I. This was followed by an abrupt, step-like increase in conductance or *membrane breakdown* which occurred at voltage V_B. When gigaohm level seal resistances were obtained, the conductance overshoot upon breakdown was slower in time course. The small step (and subsequent constant offset) in the current at the onset of the voltage ramp was due to system capacitance (primarily glass pipette), C, according to the relation $I_{Offset} = C * dV/dt$, where dV/dt is the slope of the applied voltage ramp. This current did not interfere with the measurement of slope conductance.

rence and may not have permitted full recovery of the membrane after the initial breakdown. The results for the four cells subjected to ramp and hold waveforms were not included.

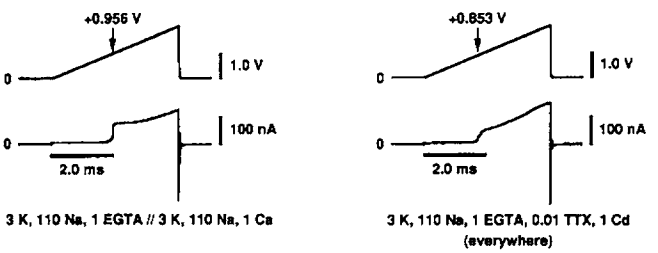

FIGURE 6 Electropermeabilization with Na^+ and Ca^{2+} channel blockers. The conductance records on the left were obtained as a control showing membrane electropermeabilization in response to a 2.0 V/4.0 ms ramp. The electrolyte bathing the second cell (*right panel*) contained TTX and Cd^{2+} (sodium and calcium channel blockers, respectively) at the concentrations noted within the figure. The presence of these channel blockers did not alter the response of the frog cardiac membrane patch. The threshold transmembrane breakdown potentials are noted on the voltage traces (*upper waveforms*); the conductance increases were 1.4 → 76.0 nS and 1.3 → 91.8 nS, left and right panels, respectively.

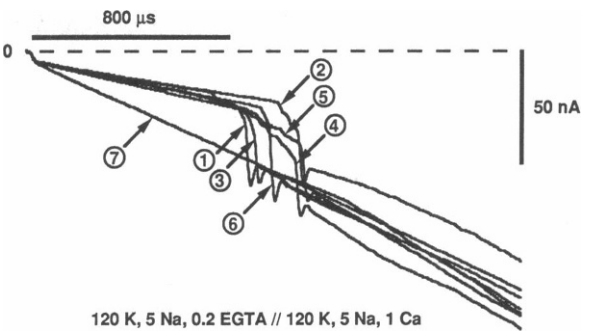

FIGURE 7 Recovery of electropermeabilized membrane patches. Shown are the current responses to seven consecutive shocks (−2.0 V/7.0 ms) that were applied to the same patch (voltage waveforms not shown). The first six shocks were applied with a 1 min intershock delay and demonstrate the recovery of the membrane patch following electropermeabilization. The seventh shock was applied within 15 s after the sixth shock and indicated that the membrane was still in a permeabilized, elevated conductance state. In each of the first six shocks the conductance doubled from ~45 to 96 nS.

The transmembrane breakdown potential is plotted vs. ramp rate, dV/dt, for the 51 cells exposed to volt-level ramps in this study (Fig. 9). The breakdown potential was weakly dependent on the rate of change of the transmembrane potential for these ramp rates as indicated by a least squares linear regression fit to the data (line not shown): $V_{breakdown} = 0.75 + 0.10 * dV/dt$, with dV/dt ranging from 0.1 to 1.0 ($R^2 = 0.5\%$). The dependence of breakdown potential on the polarity of the

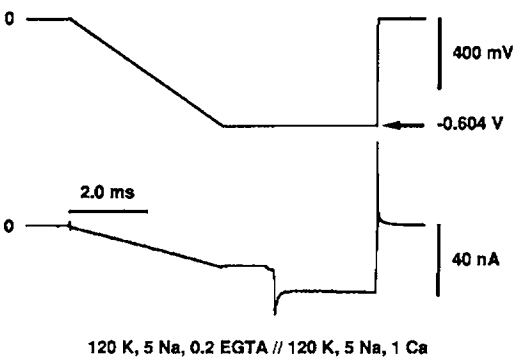

FIGURE 8 Electropermeabilization during a constant membrane potential. Electropermeabilization occurred at holding potentials of 0.4–1.1 V in four cells studied using ramp and hold waveforms. In this patch, breakdown occurred ~1 ms after a −0.6 V/4.0 ms ramp and rapidly achieved a new steady-state conductance. These observations may imply a probabilistic nature for electropermeabilization as a function of transmembrane potential. The conductance increased from 37 to 62 nS as a result of this shock. The fine structure of membrane electropermeabilization that we identified using the ramp waveform (i.e., instability preceding the step increase) was also observed with this shock protocol.

TABLE 1 **Mean first shock breakdown potential vs. bath and pipette electrolyte compositions for the macro-patch and micro-patch methods**

BATH	PIPETTE	MACRO	MICRO
mM	*mM*	*V*	*V*
Extra/1 Ca^{2+}	Extra/1 Ca^{2+}	0.523 ± 0.05, $n = 2$	0.272, $n = 1$
	Extra/0.2–0.5 EGTA	—	0.892 ± 0.13, $n = 3$;
		—	−0.825 ± 0.22, $n = 9$
Extra/1–10 EGTA	Extra/1 Ca^{2+}	—	0.888 ± 0.12, $n = 5$
Extra/1 EGTA,	Extra/1 EGTA,	—	0.825 ± 0.22, $n = 3$;
0.01 TTX, 1 Cd^{2+}	0.01 TTX, 1 Cd^{2+}	—	−0.651, $n = 1$
Intra/1 Ca^{2+}	Intra/1 Ca^{2+}	—	−0.714, $n = 1$
Intra/0.1–0.2 EGTA	Intra/0.1–2.0 Ca^{2+}	0.730 ± 0.14, $n = 5$;	0.956 ± 0.68, $n = 2$;
		−0.715 ± 0.38, $n = 9$	−0.777 ± 0.30, $n = 9$
	Intra/1 EGTA	—	1.536, $n = 1$
Extracellular = 3 K^+, 115 Na^+		Intracellular = 130 K^+, 5 Na^+	

The membrane breakdown thresholds reported in this table are for the first suprathreshold shock applied to the membrane patch (i.e., each cell contributes one data point). The data are grouped according to ramp polarity but are not sorted with respect to ramp rate.

applied voltage ramp is plotted in Fig. 10 which shows the median, 95% confidence interval, upper and lower quartile, and range of breakdown potentials. The statistical significance of the dependence of the mean breakdown potential (μ_i) on the: (*a*) patch type, (*b*) achievement of a micro-patch gigaohm level seal, and (*c*) polarity of the applied voltage ramp was determined using a *t*-test analysis. The results are presented in Table 2, where *p* is the significance test of the null hypothesis $\mu_1 = \mu_2$. We found that the difference in mean breakdown potential was not statistically significant for any of these cases, which comes as a result of the considerable variance observed in the results.

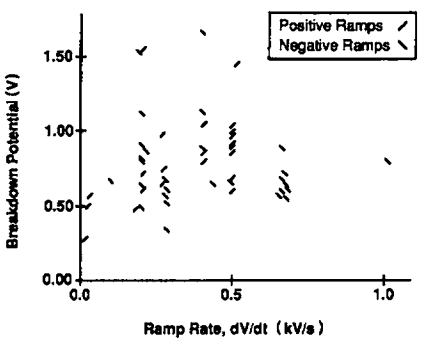

FIGURE 9 Membrane breakdown potential vs. ramp rate. The breakdown potentials for the entire 51 cell data base are plotted as a function of the velocity of the applied voltage ramp, d*V*/d*t*. In terms of overall statistics we observed only a weak dependence of the breakdown potential on the time rate of change of membrane potential over this range of velocities (0.1–1.0 kV/s). This relationship is consistent with the theory that membrane breakdown is primarily a threshold transmembrane potential phenomenon at these charging rates.

DISCUSSION

The electropermeabilization of amphibian cardiac cell membranes has been measured with volt-level ramps in transmembrane potential using the cell-attached patch

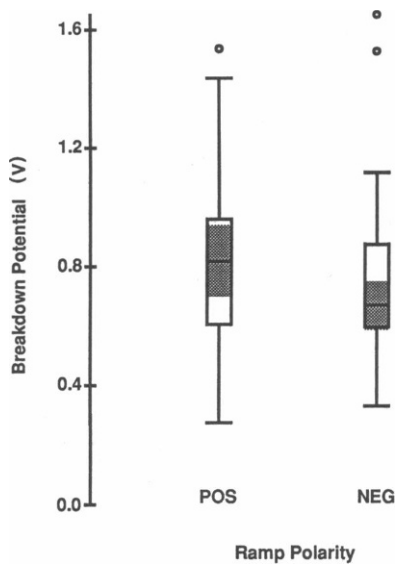

FIGURE 10 Membrane breakdown potential vs. ramp polarity. The 51 cell database was sorted on ramp polarity to compare the median (*center line*), 95% confidence interval (*shaded region*), upper and lower quartile (*open box*), and range of breakdown potentials (*upper and lower lines*). Open circles are statistical outliers. Having determined that the breakdown potential was approximately independent of the ramp velocity (Fig. 9), we analyzed its dependence on shock polarity alone. A *t*-test analysis indicated that there was no significant difference in means which are reported in Table 2 ($p > 0.53$).

TABLE 2 **A *t*-test analysis of the significance of the difference observed in the breakdown potential means for three parameters (null hypothesis: $\mu_1 = \mu_2$)**

Parameter	$\mu_1 \pm \sigma_1$	$\mu_2 \pm \sigma_2$	p
	V	*V*	
Macro-patch	$0.696 \pm 0.29, n = 16$	—	
Micro-patch	—	$0.831 \pm 0.28, n = 35$	>0.12
Seal $\geq 10^9\Omega$	$0.860 \pm 0.18, n = 9$	—	
Seal $< 10^9\Omega$	—	$0.821 \pm 0.31, n = 26$	>0.72
Positive ramps	$0.818 \pm 0.30, n = 22$	—	
Negative ramps	—	$0.766 \pm 0.29, n = 29$	>0.53

The statistical significance of the difference in mean membrane breakdown potential (μ) for (*a*) the different patch types, (*b*) the achievement of a micro-patch gigaohm seal, and (*c*) the different ramp polarities is presented based on a *t*-test analysis. In this table p is the probability that the null hypothesis $\mu_1 = \mu_2$ is true.

clamp approach. Two phases of membrane conductance change were identified, each associated with a transmembrane potential threshold. Associated with the first threshold was an increase in the noise and magnitude of the pipette current as the membrane patch began to conduct (see the I_{Cell} pathway in Fig. 1). We title this initial phase *membrane instability* and believe that it is due to the stochastic formation of conducting pores or membrane defects. A similar phenomenon has been observed in bilayer lipid membranes by Abidor et al. (1979) and others. Membrane instability occurred at a mean transmembrane potential of ~0.5 V and was followed by a rapid ($\Delta t < 30$ μs) jump in current which corresponded to a step increase in the patch conductance. We interpret this second, brief phase as *membrane breakdown* and believe that it is due to the rapid expansion of pores when the energy barrier for the formation of hydrophilic pores is overcome (Glaser et al., 1988; Weaver and Powell, 1989). Membrane breakdown occurred at a mean transmembrane potential of ~0.8 V in response to the 0.1–1.0 kV/s ramps. Because the bandwidth of our system was 30 KHz and therefore would limit step responses to ~30 μs, the transition in conductance may actually occur in less time (i.e., breakdown is a *faster* event). Indeed, Benz and Zimmermann (1980) reported pore formation within 10 ns in both bilayer lipid membranes and algal cells; also, Kinosita et al. (1988), using voltage-sensitive fluorescent dyes, reported submicrosecond pore formation in human erythrocytes.

Linearly increasing electric fields also were used by Kinosita and Tsong (1979) and Zimmermann et al. (1980*b*) to study electropermeabilization. Zimmermann et al. (1980*b*) superimposed a 286 kV/s ramp on a DC cell sizing potential to induce breakdown during the ~100 μs transit time of each cell passing through the orifice of a Coulter counter system. This technique provided cell volume, breakdown potential, and internal conductivity information; however, it did not provide details of breakdown conductance kinetics. Comparing ~6 and 24 kV/s ramps, Kinosita and Tsong reported that the voltage-induced permeability changes of a suspension of human erythrocytes occurred at the same voltage, suggesting that electroporation was strictly dependent on the *instantaneous* transmembrane potential and not its time derivatives. Our findings also suggest that the breakdown potential in amphibian cardiac cell membrane is independent of the rate of change of membrane potential across ramp rates of 0.1 to 1.0 kV/s (Fig. 9). Furthermore, these results are consistent with those of a charge-pulse study using both algal cells and bilayer lipid membranes which showed an inverse dependence of breakdown potential on charging time at rates of 100 kV/s to 10 MV/s, but a nondependence above and below these charging rates (Benz and Zimmermann, 1980). However, the statistical nature of the cell-to-cell data as suggested by Figs. 9 and 10 should be acknowledged because it undermines generalizations based on the entire cell population. For example, the least squares linear regression of the breakdown thresholds reported in Fig. 9 resulted in an $R^2 \ll 1.0$, indicating a weak fit to the data.

Our use of voltage ramps was directed at revealing membrane conductance changes *during* electropermeabilization. Patch clamp systems exhibit a limited bandwidth when compared with that offered, for example, by the charge-pulse technique, but do offer conductance measurements during the application of shock pulses. The selection of ramp waveshape voltage pulses was a means of accommodating the bandwidth limitations without sacrificing valuable experimental information. Ramp waveshapes have no discontinuity in voltage, and therefore through their use we avoided the generation of current spikes that would arise from intrinsic capacitance (primarily at the glass pipette tip). If rectangular waveshapes had been used, the resultant current spike generated on the command pulse upstroke could have masked the microsecond dynamics of conductance change during electropermeabilization. Another disadvantage of using the rectangular waveshape in conductance-based studies of electropermeabilization was the possibility of membrane conditioning by subthreshold shocks. Abidor et al. (1979) reported a dependence of breakdown kinetics in bilayer lipid membranes on electrical pretreatment. Because the resealing and characteristic recovery times after membrane breakdown in amphibian cardiac myocytes were unknown, the repetitive application of rectangular shocks in search of break-

down thresholds could alter the results. By applying a *single* high intensity ramp, the breakdown threshold could be determined, the kinetics of membrane conductance change unmasked, and the issue of electrical conditioning avoided.

Increased membrane conductance in nonmuscle cells owing to electropermeabilization has been attributed to the modulation of integral transport proteins (Tsong, 1989) and to electrically induced pores in the lipid matrix (Benz and Conti, 1981*a*) or at the lipid-protein interface (Deuticke and Schwister, 1989). The nonlinear changes in conductance of the cardiac cell membrane identified, for example, in Fig. 5 might arise from a voltage-dependent activation of the fast sodium or calcium ion channels. However, electropermeabilization in the presence of Na^+ and Ca^{2+} channel blockers (Fig. 6, *right panel*) remains characteristically unperturbed. Data on polarity independence across the membrane patch would further support the notion that channel activation, which is asymmetric around the resting potential, was not a major factor. Fig. 10 is a plot of the median breakdown potential for positive and negative ramps across the entire cell population. The difference in the means (reported previously with the results) for the positive and negative ramps was not statistically significant (*t*-test, $p > 0.53$), however, our results exhibited a statistical variance greater than twice the normal resting potential, which may mask any asymmetry that might exist (refer to Table 2).

While the resealing time after breakdown in artificial lipid bilayers is only a few microseconds (Benz and Zimmermann, 1981), that for cell membranes is on the order of seconds and minutes (Kinosita and Tsong 1977; Zimmermann et al., 1980*a*), reported also in our results (Fig. 7). This suggests that the compositional difference between artificial bilayer membranes and cell membranes has a functional effect. For example, cholesterol is a necessary constituent in all excitable cell membranes (6–50 mol percent of the total lipid pool [Adelman, 1971]). The cholesterol molecule inserts itself into the lipid bilayer in a highly specific fashion which reduces the lateral diffusion coefficient of the lipids (Houslay and Stanley, 1982). This would have the effect of increasing the time required for reorganization of the lipid molecules in a process such as membrane resealing subsequent to electropermeabilization (Sugar et al., 1987). Likewise, all other molecules associated with cell membranes such as channels, pumps, enzymes, receptors, and carbohydrates (Stryer, 1988) would depress the diffusion coefficient of membrane lipids. In eucaryotic cells there is the added consideration of the interaction between the internal cytoskeleton structure and the cell membrane. The cytoskeleton scaffolding is anchored to selected membrane proteins, rendering these molecules "immobile" (Alberts et al., 1989). The distribution of these "fixed" sites throughout the membrane may have an inhibitive effect on the net diffusive mobility of other membrane molecules and therefore also increase the time for reorganization (relaxation) of the defects that caused the increased membrane conductance (i.e., increase the resealing time). It is our belief that the difference in resealing times observed in lipid bilayers and cell membranes can be accounted for by these compositional and structural differences.

One issue of concern was the constancy of the membrane-pipette seal. A mechanical shock wave resulting from bubble formation at the surface of the Ag-AgCl metal electrode inside the pipette owing to high current density could act to dislodge the cell patch. This could alter the integrity of the membrane/pipette seal and would appear as an increase in pipette conductance. However, the maximum electrode current density used in our experiments (peak pipette current/minimum electrode surface area = 1.5 $\mu A/0.075\ cm^2 = 20\ \mu A/cm^2$) was four orders of magnitude below the threshold for bubble formation via electrolysis for platinum electrodes in Ringer's solution tested in our lab (N. Sliz and L. Tung, unpublished results), and six orders of magnitude below the threshold for electrolysis at similar pulse durations (< 20 ms) in bovine blood (Bardy et al., 1988). Also, any shock wave effects of bubble formation would have been attenuated by two factors: (*a*) the pipette contained a volume of air which acts as a mechanical compliance; sudden pressure changes would be suppressed, just as instantaneous voltage changes across a capacitor are suppressed. (*b*) The slight negative pressure (suction) applied to the pipette when the cell was mounted was maintained during the conductance measurement; this would prevent the development of a net positive pressure in the closed system. Therefore we conclude that the membrane-pipette seal remained mechanically undisturbed throughout the application of shock pulses during all of our experimental protocols.

The considerable cell-to-cell variation which we observed in breakdown potential may reflect an intrinsic statistical variance in the nature of this phenomenon (Chernomordik et al., 1987) or may reflect a variation in the morphology of the membrane patch (i.e., different surface area, different populations and mappings of sodium, potassium, and calcium channels, ion pumps, etc.). For example, although the difference in the mean breakdown thresholds reported in Table 2 were sizeable, they were not statistically significant. Additionally, the cell-attached patch clamp technique which we used may have subjected the membrane patch to a considerable mechanical stress. Because membrane breakdown involves electromechanical coupling, one must consider the contribution the added mechanical surface tension

may have on breakdown thresholds (i.e., does it lower the energy barrier for the formation or expansion of pores?). The application of an electric field exerts additional stresses on the membrane, either as electrocompressive forces (Crowley, 1973; Benz et al., 1979), surface waves (Dimitrov, 1984; Dimitrov and Jain, 1984), or an expanding pressure within the pores (Weaver and Powell, 1989). Needham and Hochmuth (1989) have reported that failure of the membrane does not depend on the mode by which a membrane is stressed (electrical, mechanical, thermal, chemical, etc.) and have demonstrated an inverse relationship between applied membrane tension and critical voltage for membrane permeabilization. Zimmermann et al. (1977) have also demonstrated an inverse relationship between cell turgor pressure and critical transmembrane breakdown voltage. Therefore the cell-to-cell variation in observed breakdown potential may also reflect variation in mechanical tension applied to each membrane patch. This variation could arise from different pipette aperture diameters (a new pipette was used for each cell) and varying degrees of suction applied to the pipette. A dependence of electropermeabilization potential threshold on mechanical stress is particularly significant for cardiac tissue because we expect cardiac cells in situ to support varying degrees of membrane tension during the active and passive phases of the cardiac cycle. Other factors that may have influenced the observed breakdown potential include the morphological condition of the membrane after the cell isolation process and the ionic make-up of the electrolyte solutions (total ionic strength, osmolarity). However, our base of experimental information was not sufficiently large and varied to determine the extent of any correlation between these variables and the electropermeabilization threshold.

We thank Doug C. Price for his help in processing the data.

This work was supported by a grant from the Whitaker Foundation.

Received for publication 10 October 1990 and in final form 18 January 1991.

REFERENCES

Abidor, I. G., V. B. Arakelyan, L. V. Chernomordik, Yu. A. Chizmadzhev, V. F. Pastushenko, and M. R. Tarasevich. 1979. Electric breakdown of bilayer lipid membranes: I. The main experimental facts and their qualitative discussion. *Bioelectrochem. Bioenerg.* 6:37–52.

Adelman Jr., W. J. 1971. Biophysics and Physiology of Excitable Membranes. Van Nostrand Reinhold Company, New York. 527 pp.

Alberts, B., D. Bray, J. Lewis, M. Raff, K. Roberts, and J. D. Watson. 1989. Molecular biology of the cell. 2nd edition. Garland Publishing, Inc, New York. 289–291, 613–681, 822–823.

Bardy, G. H., and P. Sawyer. 1990. Biophysical and anatomical considerations for safe and efficacious catheter ablation of arrhythmias. *Clin. Cardiol.* 13:425–433.

Bardy, G. H., F. Coltorti, R. B. Stewart, H. L. Greene, and T. D. Ivey. 1988. Catheter-mediated electrical ablation: the relation between current and pulse width on voltage breakdown and shock-wave generation. *Circ. Res.* 63:409–414.

Benz, R., and F. Conti. 1981*a*. Reversible electrical breakdown of squid giant axon membrane. *Biochim. Biophys. Acta.* 645:115–123.

Benz, R., and F. Conti. 1981*b*. Structure of the squid axon membrane as derived from charge-pulse relaxation studies in the presence of absorbed lipophilic ions. *J. Membr. Biol.* 59:91–104.

Benz, R., and U. Zimmermann. 1980. Relaxation studies on cell membranes and lipid bilayers in the high electric field range. *Bioelectrochem. Bioenerg.* 7:723–739.

Benz, R., and U. Zimmermann. 1981. The resealing process of lipid bilayers after reversible electrical breakdown. *Biochim. Biophys. Acta.* 640:169–178.

Benz, R., F. Beckers, and U. Zimmermann. 1979. Reversible electrical breakdown of lipid bilayer membranes: a charge-pulse relaxation study. *J. Membr. Biol.* 48:181–204.

Bhatt, D. L., D. C. Gaylor, and R. C. Lee. 1990. Rhabdomyolysis due to pulsed electric fields. *Plast. Reconstr. Surg.* 86:1–11.

Bliss, J. G., G. I. Harrison, J. R. Mourant, K. T. Powell, and J. C. Weaver. 1988. Electroporation: the population distribution of macromolecular uptake and shape changes in red blood cells following a single 50 μs square wave pulse. *Bioelectrochem. Bioenerg.* 20:57–71.

Chang, D. C., and T. S. Reese. 1990. Changes in membrane structure induced by electroporation as revealed by rapid-freezing electron microscopy. *Biophys. J.* 58:1–12.

Chassy, B. M., and J. L. Flickinger. 1987. Transformation of *Lactobacillus casei* by electroporation. *FEMS (Fed. Eur. Microbiol. Soc.) Microbiol. Lett.* 44:173–177.

Chernomordik, L. V., S. I. Sukharev, S. V. Popov, V. F. Pastushenko, A. V. Sokirko, I. G. Abidor, and Y. A. Chizmadzhev. 1987. The electrical breakdown of cell and lipid membranes: the similarity of phenomenologies. *Biochim. Biophys. Acta.* 902:360–373.

Crowley, J. M. 1973. Electrical breakdown of bimolecular lipid membranes as an electromechanical instability. *Biophys. J.* 13:711–724.

Deuticke, B., and K. Schwister. 1989. Leaks induced by electrical breakdown in the erythrocyte membrane. *In* Electroporation and Electrofusion in Cell Biology. E. Neumann, A. E. Sowers, and C. A. Jordan, editors. Plenum Press, New York. 127–148.

Dimitrov, D. S. 1984. Electric field-induced breakdown of lipid bilayers and cell membranes: a thin viscoelastic film model. *J. Membr. Biol.* 78:53–60.

Dimitrov, D. S., and R. K. Jain. 1984. Membrane stability. *Biochim. Biophys. Acta.* 779:437–468.

Dower, W. J., J. F. Miller, and C. W. Ragsdale. 1988. High efficiency transformation of *E. coli* by high voltage electroporation. *Nucleic Acids Res.* 16:6127–6145.

Escande-Géraud, M. L., M. P. Rols, M. A. Dupont, N. Gas, and J. Teissié. 1988. Reversible plasma membrane ultrastructural changes correlated with electropermeabilization in Chinese hamster ovary cells. *Biochim. Biophys. Acta.* 939:247–259.

Frazier, D. W., W. Krassowska, P.-S. Chen, P. D. Wolf, E. G. Dixon, W. M. Smith, and R. E. Idecker. 1988. Extracellular field required for excitation in three-dimensional anisotropic canine myocardium. *Circ. Res.* 63:147–164.

Gass, G. V., and L. V. Chernomordik. 1990. Reversible large-scale deformations in the membranes of electrically-treated cells: electroinduced bleb formation. *Biochim. Biophys. Acta.* 1023:1–11.

Glaser, R. W., S. L. Leikin, L. V. Chernomordik, V. F. Pastushenko, and A. I. Sokirko. 1988. Reversible electrical breakdown of lipid bilayers: formation and evolution of pores. *Biochim. Biophys. Acta.* 940:275–287.

Gross, D., L. M. Loew, and W. W. Webb. 1986. Optical imaging of cell membrane potential changes induced by applied electric fields. *Biophys. J.* 50:339–348.

Hamill, O. P., A. Marty, E. Neher, B. Sakmann, and F. J. Sigworth. 1981. Improved patch-clamp techniques for high-resolution current recording from cells and cell-free membrane patches. *Pfluegers Arch. Eur. J. Physiol.* 391:85–100.

Houslay, M. D., and K. K. Stanley. 1982. Dynamics of Biological Membranes: Influence on Synthesis, Structure and Function. John Wiley & Sons Ltd., New York. 330 pp.

Jeltsch, E., and U. Zimmermann. 1979. Particles in a homogeneous electric field: a model for the electrical breakdown of living cells in a Coulter counter. *Bioelectrochem. Bioenerg.* 6:349–384.

Jones, J. L., E. Lepeschkin, R. E. Jones, and S. Rush. 1978. Response of cultured myocardial cells to countershock-type electric field stimulation. *Am. J. Physiol.* 235:H214–H222.

Jones, J. L., C. C. Proskauer, W. K. Paull, E. Lepeschkin, and R. E. Jones. 1980. Ultrastructural injury to chick myocardial cells in vitro following "electric countershock." *Circ. Res.* 46:387–394.

Jones, J. L., R. E. Jones, and G. Balasky. 1987. Microlesion formation in myocardial cells by high-intensity electric field stimulation. *Am. J. Physiol.* 253:H480–H486.

Kinosita Jr., K., and T. Y. Tsong. 1977. Formation and resealing of pores of controlled sizes in human erythrocyte membrane. *Nature (Lond.).* 268:438–441.

Kinosita Jr., K., and T. Y. Tsong. 1979. Voltage-induced conductance in human erythrocyte membranes. *Biochim. Biophys. Acta.* 554:479–497.

Kinosita Jr., K., I. Ashikawa, N. Saita, H. Yoshimura, H. Itoh, K. Nagayama, and A. Ikegami. 1988. Electroporation of cell membrane visualized under a pulsed-laser fluorescence microscope. *Biophys. J.* 53:1015–1019.

Klee, M., and R. Plonsey. 1976. Stimulation of spheroidal cells—the role of cell shape. *IEEE (Inst. Electr. Electron. Eng.) Trans. Biomed. Eng.* BME-23:347–354.

Krassowska, K., D. W. Frazier, T. C. Pilkington, and R. E. Ideker. 1990. Potential distribution in three-dimensional periodic myocardium-Part II: application to extracellular stimulation. *IEEE (Inst. Electr. Electron. Eng.) Trans. Biomed. Eng.* 37:267–284.

Lee, R. C., D. C. Gaylor, D. Bhatt, and D. A. Israel. 1988. Role of cell membrane rupture in the pathogenesis of electrical trauma. *J. Surg. Res.* 44:709–719.

Lepeschkin, E., H. C. Herrlich, S. Rush, J. L. Jones, and R. E. Jones. 1980. Cardiac potential gradients between defibrillation electrodes. *Med. Instru.* 14:57*a*. (Abstr.)

Mehrle, W., R. Hampp, and U. Zimmermann. 1989. Electric pulse induced membrane permeabilisation. Spatial orientation and kinetics of solute efflux in freely suspended and dielectrophoretically aligned plant mesophyll protoplasts. *Biochim. Biophys. Acta.* 978:267–275.

Mir, L. M., H. Banoun, and C. Paoletti. 1988. Introduction of definite amounts of nonpermeant molecules into living cells after electropermeabilization: direct access to the cytosol. *Exp. Cell Res.* 175:15–25.

Mitra, R., and M. Morad. 1985. A uniform enzymatic method for dissociation of myocytes from hearts and stomachs of vertebrates. *Am. J. Physiol.* 249:H1056–H1060.

Mulligan, M. R., R. J. O'Neill, P. C. Zei, and L. Tung. 1988. Graded effects of pulsed electric fields on contractility of single heart cells. *Proc. IEEE/EMBS 10th Ann. Int. Conf. Nov. 1988, New Orleans, LA.* 902–903.

Needham, D., and R. M. Hochmuth. 1989. Electro-mechanical permeabilization of lipid vesicles: role of membrane tension and compressibility. *Biophys. J.* 55:1001–1009.

Neumann, E. 1989. The relaxation hysteresis of membrane electroporation. *In* Electroporation and Electrofusion in Cell Biology. E. Neumann, A. E. Sowers, and C. A. Jordan, editors. Plenum Press, New York. 61–82.

O'Neill, R. J., and L. Tung. 1989. The dynamic breakdown of heart cell membranes exposed to ramp increases in transmembrane potential. *Proc. IEEE/EMBS 11th Ann. Int. Conf. Nov. 1989, Seattle, WA.* 1731–1732.

Riemann, F., U. Zimmermann, and G. Pilwat. 1975. Release and uptake of haemoglobin and ions in red blood cells induced by dielectric breakdown. *Biochim. Biophys. Acta.* 394:449–462.

Serpersu, E. H., K. Kinosita, Jr., and T. Y. Tsong. 1985. Reversible and irreversible modification of erythrocyte membrane permeability by electric field. *Biochim. Biophys. Acta.* 812:779–785.

Sowers, A. E., and M. R. Lieber. 1986. Electropore diameters, lifetimes, numbers and locations in individual erythrocyte ghosts. *FEBS (Fed. Eur. Biochem. Soc.) Lett.* 205:179–184.

Stryer, L. 1988. Introduction to biological membranes. *In* Biochemistry. W. H. Freeman and Company, New York. 283–312.

Sugar, I. P., W. Förster, and E. Neumann. 1987. Model of cell electrofusion: membrane electroporation, pore coalescence and percolation. *Biophys. Chem.* 26:321–335.

Tacker Jr., W. A., and L. A. Geddes. 1980. Electrical Defibrillation. CRC Press, Boca Raton, FL. 185 pp.

Tovar, O., R. J. O'Neill, and L. Tung. 1990. Membrane conductance of frog heart cells following electropermeabilization. *Proc. Int. Conf. Electroporation Electrofusion, October 1900, Woods Hole, MA.* 27*a*. (Abstr.)

Tsong, T. Y. 1989. Electroporation of cell membranes: mechanisms and applications. *In* Electroporation and Electrofusion in Cell Biology. E. Neumann, A. E. Sowers, and C. A. Jordan, editors. Plenum Press, New York. 149–163.

Tung, L. 1990. Electrical injury to heart muscle cells. *In* Electrical Trauma: The Pathophysiology, Manifestations, and Clinical Management. R. C. Lee, E. G. Cravalho, and J. F. Burke, editors. University of Cambridge Press, Cambridge. In press.

Tung, L., and R. J. O'Neill. 1990. Electrical breakdown of cardiac cell membrane by volt-level transmembrane potentials. *Biophys. J.* 57: 137*a*. (Abstr.)

Weaver, J. C., and K. T. Powell. 1989. Theory of electroporation. *In* Electroporation and Electrofusion in Cell Biology. E. Neumann, A. E. Sowers, and C. A. Jordan, editors. Plenum Press, New York. 111–126.

Winegrad, S. 1979. Electromechanical coupling in heart muscle. *In* Handbook of Physiology Section 2: The Cardiovascular System Volume I. Heart. R. M. Berne, N. Sperelakas, and S. R. Geiger, editors. Waverly Press, Inc., Baltimore, MD. 393–428.

Yabe, S., W. M. Smith, J. P. Daubert, P. D. Wolf, D. L. Rollins, and

R. E. Ideker. 1990. Conduction disturbances caused by high current density electric fields. *Circ Res.* 66:1190–1203.

Zimmermann, U. 1986. Electrical breakdown, electropermeabilization, and electrofusion. *Rev. Physiol. Biochem. Pharmacol.* 105:175–256.

Zimmermann, U., F. Beckers, and H. G. L. Coster. 1977. The effect of pressure on the electrical breakdown in the membranes of *Valonia utricularis*. *Biochim. Biophys. Acta.* 464:399–416.

Zimmermann, U., J. Vienken, and G. Pilwat. 1980*a*. Development of drug carrier systems: electrical field induced effects in cell membranes. *Bioelectrochem. Bioenerg.* 7:553–574.

Zimmermann, U., M. Groves, H. Schnabl, and G. Pilwat. 1980*b*. Development of a new Coulter counter system: measurement of the volume, internal conductivity, and dielectric breakdown voltage of a single guard cell protoplast of *Vicia faba*. *J. Membr. Biol.* 52:37–50.

Zimmermann, U., P. Scheurich, G. Pilwat, and R. Benz. 1981. Cells with manipulated functions: new perspectives for cell biology, medicine, and technology. *Agnew. Chem. Int. Ed. Engl.* 20:325–344.